APPLIED PHYSICS

This research presents an interleaved bi-directional non-inverting buck-boost converter designed for public electric vehicle battery swapping stations (BSS). This study solves the critical problem of BSS vulnerability to main power outages, which threatens their operational reliability. The developed solution is a device that not only performs efficient charging but also functions as an emergency power source, utilizing power from connected batteries during a grid failure. The methodology incorporates an interleaved topology and a multi-stage constant current (MSCC) charging method controlled by a fuzzy logic controller (FLC). Experimental results show the interleaved operation successfully increased power capacity up to 1.1 kW, achieving an average efficiency of 93.44%. A distinctive feature of the result is the reduction of the output current ripple by 47.7% down to 0.92%. This is explained by the ripple-cancellation effect inherent to the interleaved design, which is a key feature for preserving long-term battery health. Furthermore, the MSCC method achieved a 13.7% reduction in execution time compared to the conventional constant current-constant voltage (CC-CV) method, with a total charging duration of 66.8 minutes. This validated prototype successfully demonstrated a seamless and automatic emergency mode transition during a power failure, directly answering the BSS reliability challenge. The prototype also confirmed its bidirectional functionality and seamless mode transition from standard charging to emergency power supply mode. The scope of this research provides a practical and high-performance integrated solution for BSS, effectively addressing vulnerability issues by improving reliability and charging time efficiency, ensuring continuous service

Keywords: battery swapping station, multi stage constant current, interleaved bidirectional converter

UDC 62
DOI: 10.15587/1729-4061.2025.342160

IMPLEMENTATION OF INTERLEAVED BI-DIRECTIONAL DC-DC CONVERTER WITH MULTI STAGE CONSTANT CURRENT CHARGING BASED ON FUZZY CONTROL FOR DISTURBANCE-RESISTANT ELECTRIC VEHICLE BATTERY SWAPPING STATIONS

Sonki Prasetya
Doctor, Associate Professor
Department of Mechanical Engineering
Researcher of Center for Conversion Conservation and Appliend Renewable Energies (CARE)*
Eka Prasetyono
Corresponding author
Master of Electrical Engineering**
E-mail: eka@pens.ac.id
Mochamad Ari Bagus Nugroho
Master of Electrical Engineering**
Epyk Sunarno
Master of Electrical Engineering**
Muhammad Fikri Rizki
Bachelor of Electrical Engineering**
Department of Electrical Engineering
Haolia Rahman
PhD, Doctor, Associate Professor
Department of Mechanical Engineering*
Muhammad Hidayat Tullah
Magister, Lecturer
Department of Mechanical Engineering*
Jazuli Fadil
Doctor of Electrical Engineering
Department of Electrical Engineering***
Teguh Suprianto
Doctor of Mechanical Engineering
Department of Mechanical Engineering***
Lauhil Mahfudz Hayusman
Master of Electrical Engineering
Department of Electrical Engineering***
*Politeknik Negeri Jakarta
Prof. DR. G. A. Siwabessy str., Depok, West Java, Indonesia, 16424
**Department of Electrical Engineering
Politeknik Elektronika Negeri Surabaya
Raya ITS str., Kecamatan Sukolilo, Kota Surabaya, Jawa Timur, Indonesia, 60111
***Politeknik Negeri Banjarmasin
Brig Jend. Hasan Basri str., Pangeran, Kec. Banjarmasin Utara, Kota Banjarmasin, Kalimantan Selatan, Indonesia, 70124

Received 04.08.2025
Received in revised form 08.10.025
Accepted 17.10.2025
Published 31.10.2025

How to Cite: *Prasetya, S., Prasetyono, E., Nugroho, M. A. B., Sunarno, E., Rizki, M. F., Rahman, H., Tullah, M. H., Fadil, J., Suprianto, T., Hayusman, L. M. (2025). Implementation of interleaved bi-directional DC-DC converter with multi stage constant current charging based on fuzzy control for disturbance-resistant electric vehicle battery swapping stations. Eastern-European Journal of Enterprise Technologies, 5 (5 (137)), 6–18. https://doi.org/10.15587/1729-4061.2025.342160*

1. Introduction

The massive and global trend of electric vehicle adoption requires supporting infrastructure, such as charging stations. However, conventional charging has the disadvantage of long charging times [1, 2]. This has led to solutions like public electric vehicle battery swapping stations (BSS) [3]. These stations

let users swap their empty batteries for full ones. This makes electric vehicles able to travel farther. This system provides an alternative to charging electric vehicle batteries. It is especially useful for electric motorcycles, the aim is to improve user time efficiency.

Trust in infrastructure is contingent on the operational reliability of the infrastructure itself [4]. Battery swapping stations can be powered by the grid or by integrating new renewable energy sources [5, 6]. Nonetheless, there is a possibility that both of these primary power sources could encounter temporary interruptions or even total loss of power. This is a critical weakness in the BSS network. Ideally, battery swapping stations should always be supplied with primary power sources so that fully charged batteries can be provided for customers to swap. Occurrence of an outage or blackout at the primary power source of a battery swapping station would result in the station's inability to provide fully charged batteries to customers. This would undoubtedly prove to be exceedingly disadvantageous to customers, particularly with regard to the amount of time it would entail.

The development of electric vehicle charging infrastructure has driven intensive research into efficient and flexible power converter topologies. Among the various technologies available, bidirectional DC-DC converters have established themselves as key components, demonstrated to facilitate bidirectional power flow between vehicles and the power grid. The use of this architecture has been validated in various studies; optimization of fast charging architecture using fuzzy logic control has been focused on to improve performance [7]. Meanwhile, a technique for improving the transition of operating mode in bidirectional converters has also been presented, which underlines the importance of operational smoothness in such systems [8].

Specifically, the non-inverting buck-boost converter topology has been analyzed as a compact and effective solution for applications requiring the ability to step up and step down voltage without reversing polarity. The application of this topology has been demonstrated for fuel cell applications, proving its flexibility in managing different power sources [9]. Furthermore, the design of this converter has been specifically analyzed and simulated for battery charging applications, confirming its suitability for use in power charging systems [10]. Support for the fundamental role of this topology is reinforced by a comprehensive review that positions advanced DC-DC converters as the core of fast charging systems integrated with battery storage [11]. Additionally, an efficient non-inverting buck-boost converter design with enhanced step-up/down capability has been specifically presented, proving that this topology continues to be the subject of active innovation to achieve higher performance [12].

Therefore, studies that are devoted to enhancing the operational reliability and addressing the vulnerabilities of BSS infrastructure are of significant scientific relevance.

2. Literature review and problem statement

Trust in an infrastructure is highly dependent on its operational reliability, an aspect emphasized in a review of mobile charging station technology [4]. However, it has been shown that the majority of existing research has not specifically addressed the challenge of operational vulnerability in BSS due to power outages from the main source. Adaptive charging strategies and optimal sizes for BSS have been discussed, but solutions to maintain service continuity in the event of a total failure of the power source have not been directly provided [3].

The reason for this is likely because the main focus of research tends to be on the integration of alternative energy sources. For example, there have been studies focusing on the implementation of renewable energy-based charging stations to increase energy independence [5]. Similarly, an open-source hardware platform for power electronics that supports renewable power generation and energy storage has also been presented [6]. Although these approaches are valuable, renewable energy sources themselves are still vulnerable to interruptions or intermittency, so they do not completely eliminate the risk of power loss. Thus, a significant research gap lies in the lack of integrated system designs specifically designed as solutions to the vulnerability of BSS in order to improve reliability and resilience to disruptions in primary resources. This issue has not been widely discussed because most studies have focused more on improving the performance, efficiency, and stability of charging, rather than on the internal system resilience of the BSS itself.

One way to overcome the difficulties that have been identified is to develop an integrated system that combines superior hardware topology, efficient charging methods, and intelligent control systems. From a hardware perspective, one of the main challenges is to suppress output current ripple. The importance of this variable is emphasized in an analysis that specifically shows how current ripple in DC-DC chargers can negatively impact the health and lifespan of Li-Ion batteries [13]. The relevance of this issue in modern systems is also demonstrated in the development of the rotating phase shedding technique for interleaved converters to mitigate the thermal effects caused by current ripple during fast charging [14]. Given the importance of suppressing current ripple, an effective approach is to implement an interleaved topology [15]. The control model and digital implementation of a three-phase interleaved converter have been demonstrated for electric vehicles, confirming its suitability for high-power applications [15]. The relevance of this topology is also demonstrated in the context of renewable energy systems, where a three-phase interleaved boost converter design has proven effective for energy storage systems in photovoltaic (PV) applications [16]. Other topologies such as the cascaded bidirectional buck-boost converter have also been analyzed for battery charging applications, demonstrating the validity of its bidirectional operation [17]. In addition, a multiphase interleaved converter based on a cascaded non-inverting buck-boost topology has been specifically developed, which has proven successful in reducing the number of switching components [18]. In fact, the combination of an interleaved buck converter topology with fuzzy logic control has been proven to function as a precise current regulator for Lithium-ion battery charging applications [19]. However, these studies focus on improving converter performance for general electric vehicle applications and have not explicitly applied them in the context of emergency power supply systems designed to improve BSS resilience.

Furthermore, to overcome the long charging time weakness of the conventional CC-CV method, a new approach is needed. The inefficiency of the standard CC-CV method is primarily attributed in practical literature to its prolonged constant voltage (CV) phase, where the charging current tapers off slowly, thus significantly extending the total time required to reach full capacity [20]. Following this, specific academic studies have also focused on its improvement; for example, a multi-step profile that modifies the standard CC-CV process has been proposed specifically to shorten the overall charging duration [21]. Building upon these foundations, the

Multi-Stage constant current (MSCC) charging method can be adopted. This approach has proven its reputation for shortening charging duration, as emphasized in the context of BSS [3]. The characteristics of the MSCC process, which visually shows the stages of current decline, have been used in advanced battery models for estimating the State of Charge, confirming the validity of the charging profile [22]. The MSCC method for Li-Ion batteries was first introduced in fundamental research that proved its feasibility as a faster alternative [23]. Furthermore, an optimal charging pattern for high-performance MSCC methods has been presented, confirming that this approach is not only faster but can also be further optimized for maximum efficiency [24]. In fact, the application of state-flow-based control in the MSCC method has also been proven effective for battery chargers in two-wheeled electric vehicles [25]. However, the focus of these studies was limited to optimizing the charging process itself and did not integrate the MSCC method into a two-way hardware system capable of switching functions to supply power during emergencies.

To manage this complex and non-linear system, a modern control approach is required. A fuzzy logic controller (FLC) can be an appropriate solution, as it fundamentally works based on "IF-THEN" linguistic rules rather than precise mathematical models, as described in the basic literature on FLC [26]. The practical advantages of this approach have been proven in various applications; for example, a critical review has confirmed that FLC is superior to conventional PI controllers in the maximum power point tracking (MPPT) in photovoltaic systems, especially under varying irradiation conditions [27]. In fact, type-2 FLC has been applied to accelerate conventional CC-CV charging methods, demonstrating its success in significantly reducing charging duration compared to PI controllers [28]. Furthermore, FLC has been successfully applied as a battery charge-discharge controller in microgrid applications, proving its capability in effectively regulating bidirectional power flow [29]. Moreover, an investigation presents a balanced performance comparison, where FLC (specifically the Sugeno type) shows the most superior stability and voltage ripple, even though the PID controller is able to provide a faster rise time with a comparable overshoot level [30]. However, current FLC applications have not specifically addressed its application for precisely controlling the multi-stage constant current (MSCC) charging method, where stable transitions between charging stages are crucial for battery efficiency and health in an integrated system for BSS reliability.

Based on the above description, all of these points indicate that although each technological component, such as bidirectional converters, interleaved topologies, MSCC charging methods, and fuzzy logic controllers, has been extensively researched in its respective context, there is a clear gap in the literature. Studies on strategies for BSS have indeed been conducted, but integrated solutions for resilience against primary power source disturbances remain an unresolved issue. Thus, it can be concluded that there is no integrated DC-DC converter system design that combines fuzzy-controlled MSCC charging methods to support total charging time efficiency in BSS applications, while also supporting solutions to the problem of vulnerability in the station's primary power source. Therefore, it is considered necessary to conduct a study on the development of an enhanced non-inverting buck-boost bi-directional converter with interleaving techniques to suppress charging current ripple in order to maintain long-term battery health, specifically designed to improve the reliability and resilience of electric vehicle BSS.

3. The aim and objectives of the study

The aim of this study is to develop an interleaved bi-directional non-inverting buck-boost converter integrated with sensors and FLC embedded control as MSCC control, thereby creating a device to address the vulnerabilities of battery swapping stations as described in the previous chapter. This development enables a battery swapping station to continue providing charged batteries to users even during temporary power outages or blackouts by switching the power source to batteries connected to the battery swapping station as an emergency power source to charge several batteries.

To achieve this aim, the following objectives were accomplished:

– to verify the hardware performance of the interleaved bi-directional converter, ensuring increased power capacity and a reduction in output current ripple;

– to implement and evaluate the fuzzy logic controller (FLC) algorithm for the multi-stage constant current (MSCC) charging method to achieve charging time efficiency;

– to test the integrated system functionality to validate its bi-directional operational capability and seamless transition to emergency mode.

4. Materials and methods

The object of this study is an integrated system consisting of an interleaved bidirectional DC-DC converter, sensors, and a microcontroller. The main hypothesis of the study is the integration of this system is designed to produce low current ripple, adaptive control response at each constant current stage, and, most importantly, the ability to switch power sources when the main power source is detected to be experiencing interference. The overall architecture and flow of interaction between these components are illustrated visually in the block diagram presented in Fig. 1:

1. Hardware design.

The diagram shows that this device uses an interleaved bi-directional non-inverting buck-boost converter topology, which allows the converter to operate in two directions, both in voltage reduction mode and voltage increase mode, with the same converter polarity at each input and output. In addition, with the interleaved topology, the converter can have lower output current ripple, which is a safety requirement for charging lithium-ion batteries.

To support the converter control on this device, two current sensors and two voltage sensors are required, with one sensor located on the input side and one on the output side of the device. The current and voltage sensors provide data to the STM32 microcontroller, which acts as a data processor and controls the converter through a gate driver by sending PWM signals obtained from the sensor data processing results. This system also includes a relay as a circuit breaker when the device is operating as a charger or as a power supply. This load capacity plan describes the loads that will be used in system testing, including 72V 20Ah Li-ion battery pack, battery voltage range 63V-83V, charging current = $20 \times 0.2 = 4$ A.

The converter design planning was carried out using the calculations described in Chapter 2. There are two types of calculations for planning the converter in this system, namely the converter calculations in buck mode and boost mode. Referring to the formula described above, the converter design planning is calculated as follows.

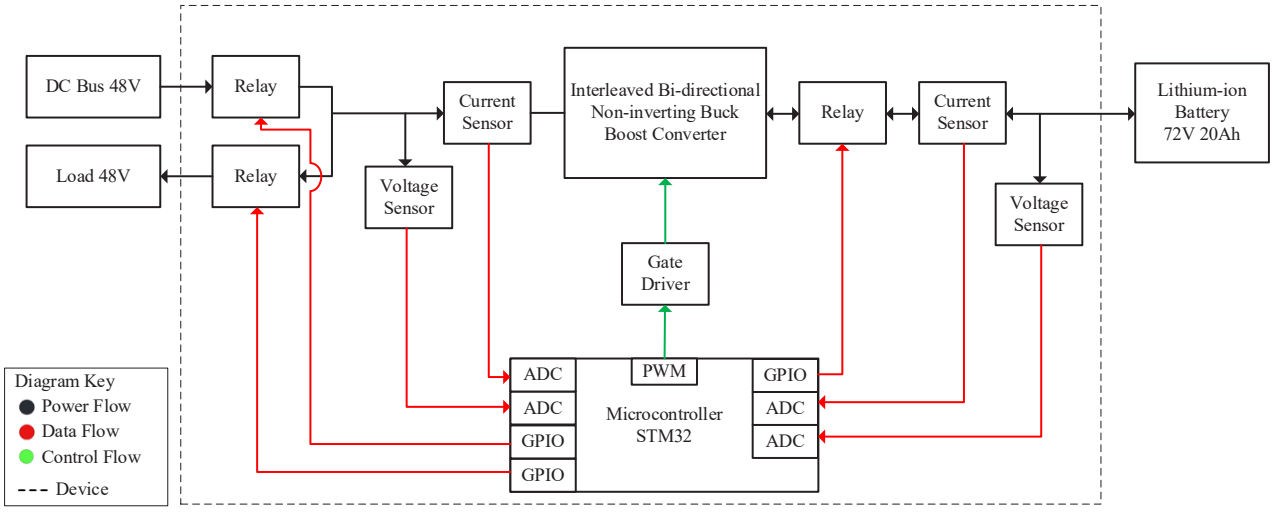

Fig. 1. Block diagram

From the results of the two modes above, it can be concluded that the inductor value used in this converter is greater than or equal to 35 μH, which is the highest value from the two calculations. As for the capacitor value, the maximum minimum value is 47 μF, so the capacitor used in this converter is greater than the maximum minimum value. For the values of the *Rg*(on), *Rg*(off), Ferrite bead, RC_{DCL}, and RC_{SN} components, refer to the recommendations in the data sheet, namely [31]:

Rg(on) = 20 Ω; *Rg*(off) = 50 Ω;

Ferrite bead = 270 Ω, 100 MHz;

RC_{DCL} = 5 Ω, 10 nF; RC_{SN} = 15 Ω, 68 pF.

Minimum microcontroller system design planning is important as the center of the system that processes data and controls the operation of the entire system. The STM32G441KBT6 microcontroller was chosen because it has a computing speed of up to 170 MHz, making it suitable for PWM signal generators that require high data execution. The input-output (I/O) used in this microcontroller consists of 4 ADCs for sensor readings and 4 timers for PWM. In addition, the STM32G441KBT6 has excellent communication capabilities through various protocols such as UART, SPI, I2C, and CAN, allowing this microcontroller to connect to external devices or additional modules to expand system functionality. With 128 kB of flash memory and 192 kB of RAM, this microcontroller is capable of storing and processing complex programs and sensor data efficiently. Another advantage is the DMA (direct memory access) feature, which speeds up data transfer between peripherals without burdening the CPU, allowing the system to work more responsively, especially in applications that require real-time sensor data acquisition and precise output control [32].

The voltage sensor design in this system is designed for a maximum measurable voltage of 120 V and a maximum V_{sense} of 250 mV. Therefore, the voltage divider resistor value is calculated as follows

$$250\ \text{mV} = \frac{R2}{R1+R2+R3} \times 120\ \text{V}.$$

Therefore, $R1$ = 1.1 MΩ, $R2$ = 3.3 kΩ, $R3$ = 1.1 MΩ.

The current sensor design in this system is designed for a maximum measurable current of 30A and a maximum V_{sense} of 250 mV. Therefore, the shunt resistor value is calculated as follows

$$250\ \text{mV} = R_{shunt} \times 30\ \text{A}.$$

Therefore, R_{shunt} = 8 mΩ.

In this study, a relay was created due to the unavailability of relays on the market with the required specifications, thus necessitating the creation of a solid state relay (SSR) using two MOSFETs and two DS-SD diodes. In addition to breaking the circuit, this relay also acts as a regulator of the desired current direction. In the design of this relay, MOSFETs from inchange semiconductor with the manufacturer code 2SK2753 were used. These MOSFETs have specifications of 120 V 50 A, making them suitable for use in this study. Meanwhile, the diodes used as MOSFET support components are from SMC Diode Solution with the manufacturer code 60CPQ150. These diodes have specifications of 150 V 60 A, making them suitable for use in this study. To make it a relay, an optocoupler is needed as a MOSFET drive component, so an optocoupler with the manufacturer code TLP512 is used.

2. Fuzzy logic controller design.

MatLab is used as computational software to design and visualize the FLC design in this study. In designing FLC, there are several things that need to be considered, such as what input variables are needed and what form of fuzzy output is desired. In this study, the input variables used are the error variable and the delta error (the difference between the current and previous errors). As for the membership function used, it is triangular because the triangular type has light computation and is sufficient to control only the current or voltage. There are 7 membership functions used, which are intended to provide the control system with a sufficient range to produce a smooth system response. The membership function range of the error variable is taken from how high the current value is used so that if the designed system can work up to a current of 20 A, the mf range used is –20 to 20. Meanwhile, the mf range of the delta error variable itself is determined by how sensitive the current increase is when the control is running, therefore, for a smooth response, the range starts from –5 to 5. The FLC output variable in this study is configured as a step value for increment

and decrement duty cycles, so that a smooth system response is determined by how high the step value output from the FLC is. Therefore, the mf range for the FLC output variable uses a range of –0.5 to 0.5. With 7 membership functions for each input and output variable, at least 49 combinations of IF THEN rules are required for the FLC.

The combination of the seven membership functions for each input and output variable produces 49 "IF-THEN" inference rules. The rule base that implements these 49 rules, which map the logical relationship between the input Error and Delta Error to the output control action, is presented in matrix form in Fig. 2.

		Delta Error						
	&&	NL	NM	NS	Z	PS	PM	PL
ERROR	NL	NL	NL	NM	NM	NS	NS	NS
	NM	NL	NM	NM	NS	NS	NS	NS
	NS	NM	NM	NS	NS	NS	NS	NS
	Z	Z	Z	Z	Z	Z	Z	Z
	PS	PS	PS	PM	PM	PM	PL	PL
	PM	PS	PM	PM	PM	PL	PL	PL
	PL	PM	PM	PM	PL	PL	PL	PL

Fig. 2. Rule base fuzzy logic controller

3. Experimental procedures used.

The testing process is the most important process in a study, requiring supporting equipment and an appropriate test setup, including procedures applied before, during, and after testing. Any differences in test conditions can lead to different test results. In this test, the supporting equipment used included a Yokogawa DL850E oscilloscope with three voltage probes and two current probes, a 48 V 30 A DC Bus, and a resistive load. Meanwhile, the main test material used was one electric motor battery with a nominal voltage of 72 V and a maximum voltage of 84 V with a capacity of 20 Ah, assuming that the battery was in normal condition. The Fig. 3 shows the position of each voltage probe and current probe.

The blue circle indicates the location of the voltage probe, while the green circle indicates the location of the current probe. Testing in this study was conducted on a laboratory scale and in an air-conditioned room with a temperature set at 24°C.

5. System implementation and experimental results

5. 1. Verification of interleaved bi-directional converter performance

As a physical realization of the proposed system design, a functional prototype has been successfully assembled. Fig. 4 shows the final form of the hardware that integrates the power converter board, sensor system, microcontroller, and gate driver into a single unit.

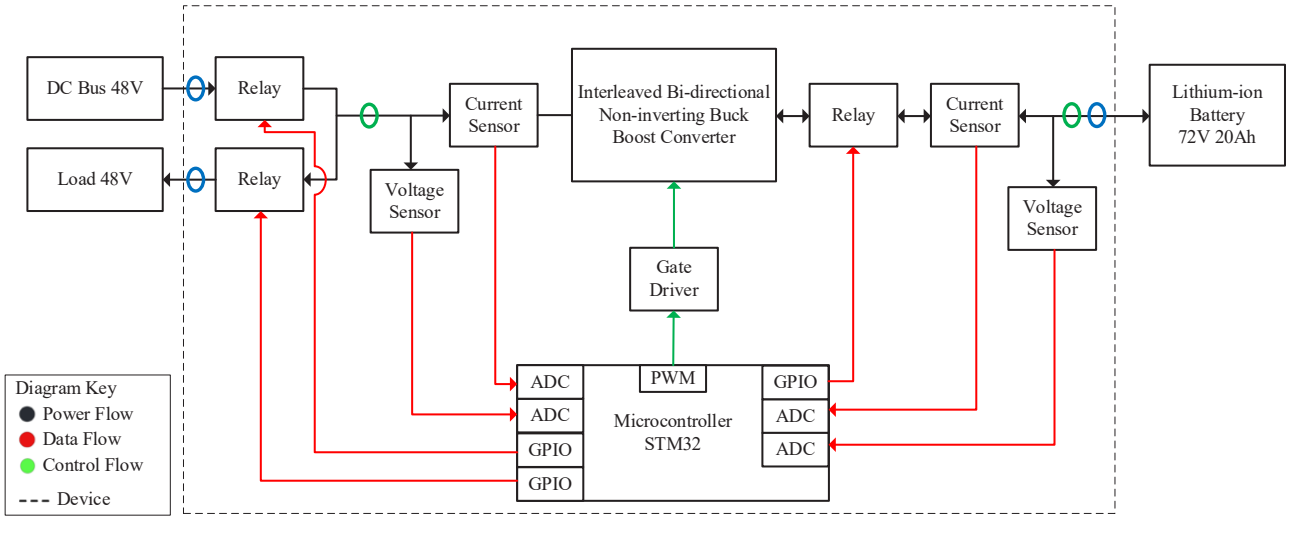

Fig. 3. Positioning probe while experiment

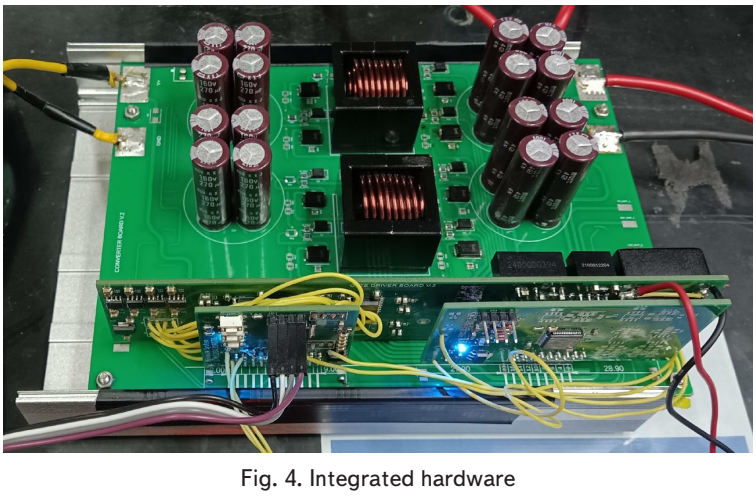

Fig. 4. Integrated hardware

With the prototype fully integrated as shown in Fig. 4, further experimental testing was conducted to validate the system's performance quantitatively.

The first stage of hardware verification was to test each converter channel separately to evaluate its performance as a single unit. Table 1 presents a summary of the average performance comparison between leg 1 and leg 2 to ensure uniform basic characteristics before operating in interleaved mode.

Table 1

Average performance comparison of leg 1 and leg 2 converters

Parameters	Converter leg 1	Converter leg 2
Average efficiency (%)	92.45	92.24
Average voltage error (%)	2.48	2.54

Based on the data summarized in Table 1, a direct comparison between the two converter legs shows very consistent and uniform basic performance. The average power conversion efficiency of both units is very comparable, namely 92.45% for leg 1 and 92.24% for leg 2, with a negligible difference of only 0.21%. Similarly, the average voltage error relative to the theoretical value also shows nearly identical values, namely 2.48% and 2.54%. This consistency in performance is very important because it confirms that the two converter units built have uniform characteristics and function according to the design. This uniformity provides a solid and valid foundation for the next testing phase, in which both units will be operated simultaneously in an interleaved configuration. In addition to performance parameters, the quality of the output signal was also evaluated for each leg. Table 2 presents a comparison of the average output ripple, which will serve as baseline data for assessing the effectiveness of ripple suppression in interleaved mode.

Table 2

Comparison of average output ripple of leg 1 and leg 2 converters

Parameters	Converter leg 1	Converter leg 2
Average current ripple (%)	1.76	2.47
Average voltage ripple (%)	2.31	2.42

Table 2 presents crucial data regarding the output signal quality of each converter leg operating individually. The measurement results show very consistent voltage ripple between the two units, namely 2.31% for leg 1 and 2.42% for leg 2, which further reinforces the finding that the two hardware units have uniform characteristics. Although there is a slight variation in the average current ripple (1.76% for leg 1 and 2.47% for leg 2), these values are still within acceptable limits for individual operation. Most importantly, this data serves as essential baseline data. This performance will be a quantitative benchmark for evaluating the effectiveness of the interleaved topology in suppressing ripple, a key parameter for maintaining health and extending battery life in the next stage of integrated system testing. After the basic characteristics of each converter unit were validated, testing proceeded to the core stage, which was to operate both legs simultaneously in an interleaved configuration. Table 3 presents comprehensive performance data from this integrated system, which aims to verify improvements in power capacity and operational efficiency.

Table 3 clearly shows the success and significant advantages of implementing the interleaved topology. The main result shows that the converter is capable of achieving a power conversion capacity of up to 1116.3 W. This value represents a 99.9% increase in power capacity compared to the best performance of the individual legs (558.06 W), which convincingly validates that the interleaving technique successfully doubles the power handling capability of the system. More importantly, this increase in capacity was achieved while maintaining very high efficiency. The average efficiency of the interleaved system was recorded at 93.44%, slightly higher than the average efficiency of the individual leg tests (~ 92.4%). This finding confirms that combining the two converter units does not cause significant power loss and actually slightly improves overall operational efficiency, proving that the proposed hardware design successfully achieves its objectives. In addition to increasing power capacity, the main objective of implementing the interleaved topology is to significantly reduce output ripple. Table 4 presents the ripple test data from the integrated system, which will be evaluated against the baseline data from the individual leg tests.

Table 3

Interleaved converter test results

Mode	Duty cycle				Vin (V)	Iin (A)	Pin (W)	Vout (V)	Vout theory (V)	Iout (A)	Pout (W)	Eff (%)	Error (%)
	Q2	Q1	Q3	Q4									
Boost	100%	0%	80%	20%	52.60	9.59	504.38	65.47	65.75	7.23	473.52	93.88	0.43
	100%	0%	75%	25%	52.51	10.82	568.00	69.50	70.01	7.69	534.27	94.06	0.73
	100%	0%	70%	30%	52.40	12.33	645.99	74.17	74.86	8.21	608.66	94.22	0.91
	100%	0%	65%	35%	52.26	14.20	742.03	79.38	80.40	8.80	698.54	94.14	1.27
	100%	0%	60%	40%	52.08	16.48	858.05	85.30	86.80	9.47	807.76	94.14	1.73
	100%	0%	55%	45%	51.81	19.44	1007.0	91.94	94.20	10.32	948.92	94.23	2.41
	100%	0%	50%	50%	51.52	23.12	1190.8	100.02	103.03	11.16	1116.3	93.74	2.92
Buck	50%	50%	100%	0%	53.19	6.05	321.80	25.74	26.60	11.29	290.55	90.29	3.20
	60%	40%	100%	0%	52.87	8.45	446.54	30.70	31.72	13.45	412.90	92.47	3.22
	70%	30%	100%	0%	52.66	11.28	593.79	35.61	36.86	15.58	554.79	93.43	3.40
	80%	20%	100%	0%	53.45	14.53	776.56	40.48	42.76	17.72	717.31	92.37	5.32
	90%	10%	100%	0%	52.20	18.07	943.24	45.16	46.98	19.69	888.97	94.25	3.87
Average												93.44	2.45

Table 4

Current and voltage ripple testing of interleaved converter

Mode	Duty cycle				Vout (V)	Iout (A)	Ip-p	Vp-p	Ripple I	Ripple V
	Q2	Q1	Q3	Q4						
Boost	100%	0%	80%	20%	65.47	7.23	0.07	1.80	0.97%	2.75%
	100%	0%	75%	25%	69.50	7.69	0.10	2.20	1.30%	3.17%
	100%	0%	70%	30%	74.17	8.21	0.09	1.80	1.10%	2.43%
	100%	0%	65%	35%	79.38	8.80	0.09	2.20	1.02%	2.77%
	100%	0%	60%	40%	85.30	9.47	0.09	2.20	0.95%	2.58%
	100%	0%	55%	45%	91.94	10.32	0.12	2.20	1.16%	2.39%
	100%	0%	50%	50%	100.02	11.16	0.13	2.20	1.16%	2.20%
Buck	50%	50%	100%	0%	25.74	11.29	0.11	1.17	0.97%	4.54%
	60%	40%	100%	0%	30.70	13.45	0.07	0.93	0.52%	3.03%
	70%	30%	100%	0%	35.61	15.58	0.10	0.70	0.64%	1.97%
	80%	20%	100%	0%	40.48	17.72	0.10	0.80	0.56%	1.98%
	90%	10%	100%	0%	45.16	19.69	0.13	0.73	0.66%	1.62%
Average									0.92%	2.62%

Table 4 presents the most significant evidence of the superiority of the interleaved topology implemented in this study. Test results show that the average output current ripple was dramatically reduced to only 0.92%. Compared to the baseline data from individual tests (where the best performance was 1.76% in leg 1), this value represents a 47.7% reduction in current ripple. This finding is particularly important because it directly validates one of the main objectives of the hardware design, namely current ripple mitigation to maintain battery health and extend battery life. The success in reducing ripple by almost half proves that the ripple-cancellation effect of interleaved operation works effectively in the built prototype.

Collectively, the test results in this sub-chapter convincingly validate that the proposed bi-directional interleaved converter hardware design has successfully achieved its main objective, which is to double the power handling capacity while significantly suppressing output current ripple. This success proves that the built prototype is a solid and reliable platform for the implementation and evaluation of control algorithms in the next stage.

5. 2. Implementation and evaluation of FLC-MSCC charging control

With a hardware platform that has been proven reliable from previous tests, the research continued with the implementation and evaluation of the control algorithm. This subchapter specifically discusses the performance of the fuzzy logic controller (FLC) designed to regulate the multi-stage constant current (MSCC) charging method to achieve charging time efficiency. In accordance with the design methodology, the FLC was developed with two input variables (error and delta error) and one output variable (duty cycle change). Fig. 5 displays the control surface of the designed FLC, which is a three-dimensional representation of the rule base that maps all possible input conditions to the corresponding control output actions.

With the validated control logic as shown by the control surface in Fig. 5, the FLC was then implemented on a hardware prototype to actively regulate the charging process using the multi-stage constant current (MSCC) method. Testing was conducted by charging the battery from its initial state to full capacity to evaluate two main parameters: the FLC's ability to maintain current stability at each stage and the total time efficiency achieved compared to conventional methods. After the FLC logic was validated, testing continued to evaluate its actual performance in regulating the charging process using the MSCC method. Table 5 summarizes the main quantitative results of this test, highlighting key parameters such as current stages, total charging time, and average efficiency achieved.

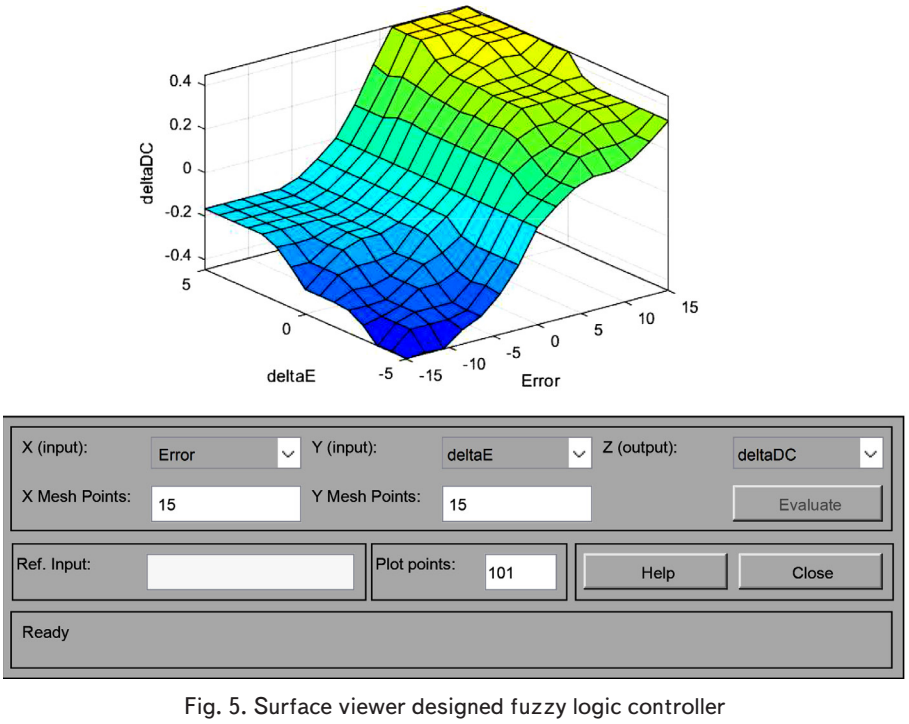

Fig. 5. Surface viewer designed fuzzy logic controller

Table 5

Summary of multi stage constant current charging test results

Parameters	Value
Cut-off voltage	83 V
Stage 1 current	4 V
Stage 2 current	2.8 A
Stage 3 current	2 A
Efficiency	91%
Total charging time	66.8 min

The test results summarized in Table 5 show that the FLC-controlled MSCC charging method successfully charged the battery to full capacity in a total time of 66.8 minutes. This time is significantly faster when compared to the conventional CC-CV method, which in a separate test took 75.1 minutes to complete the same task. This represents a time saving of 13.7%, a very significant efficiency improvement for BSS applications where battery exchange speed is a top priority. Furthermore, this charging process took place with a solid average efficiency of 91%. This success not only validates the implementation of the FLC algorithm in precisely controlling the MSCC current stages, but also proves that the proposed method effectively overcomes the duration weakness of conventional charging methods. The dynamic MSCC charging process from start to finish is illustrated in Fig. 6. This graph presents real-time changes in battery voltage V_{OUT} and I_{OUT} to visualize each stage of the charging process.

The graph in Fig. 6 visually validates the successful implementation of the FLC-controlled MSCC charging method. The blue line (I_{OUT}) clearly shows three distinct constant current stages. The process begins with a constant current of 4 A (Stage 1), which is maintained until the battery voltage (orange line, V_{OUT}) reaches the cut-off limit of 83 V at around 2900 seconds. At that point, the FLC precisely reduces the current to the next stage (~ 2.8 A), and this process repeats for the final stage (~ 2 A). Charging is completely stopped shortly after the 4000th second (66.8 minutes total) when the voltage again reaches the cut-off limit at the lowest current stage. This visualization provides strong empirical evidence that the designed FLC algorithm is capable of executing a multi-stage charging strategy stably and accurately as planned.

To validate the superiority of the MSCC method in terms of time efficiency, a comparative test was conducted with the conventional constant current-constant voltage (CC-CV) method. Fig. 7 presents a direct comparison between the two methods by displaying the voltage and current curves of each charging process simultaneously.

The comparison graph in Fig. 7 visually highlights the fundamental differences between the MSCC and CC-CV charging methods. During the initial constant current (CC) stage, both methods exhibit similar behavior, where the current is kept constant at 4 A and the battery voltage (blue and red curves) rises identically. The crucial point of difference occurs when the voltage reaches the 83 V cut-off limit. At this point, the CC-CV method (orange current) enters a long constant voltage (CV) phase, where the charging current decreases slowly and takes a significant amount of time to reach the end point. In contrast, the MSCC method (green current) avoids this inefficient CV phase by gradually decreasing the current. As seen, the MSCC method completes the entire charging process in 66.8 minutes, while the CC-CV method only finishes in 75.1 minutes. This visual comparison convincingly proves that the main advantage of MSCC lies in the elimination of the long charging "tail" from the CV phase, resulting in a total time saving of 13.7%.

Thus, the results in this sub-chapter collectively prove that the implementation of the fuzzy logic controller successfully controls the MSCC charging method effectively and achieves a significant time saving of 13.7% compared to the conventional method. After this main charging function has been validated, further testing will evaluate the full functionality of the integrated system, namely its bidirectional operational capability and transition to emergency mode.

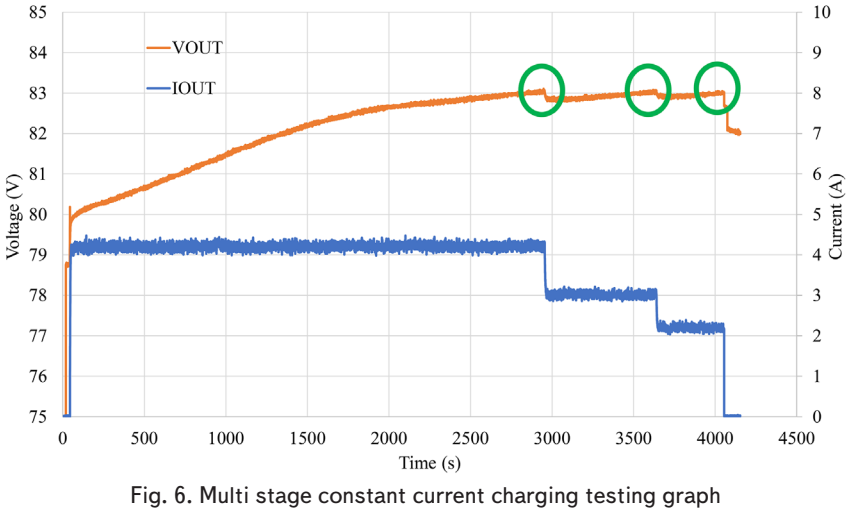

Fig. 6. Multi stage constant current charging testing graph

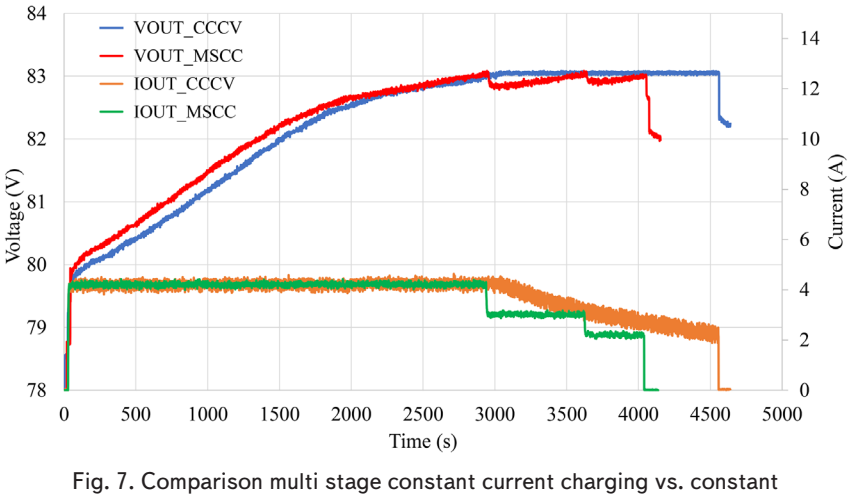

Fig. 7. Comparison multi stage constant current charging vs. constant current-constant voltage

5. 3. Integrated system functionality testing

After the performance of the converter hardware and the effectiveness of the charging control algorithm were successfully validated in the previous subsection, the final testing phase focused on evaluating the integrated system functionality. This subsection will verify two core capabilities of the developed prototype: bi-directional operational capability and smooth mode transition from normal charging conditions to emergency power supply mode.

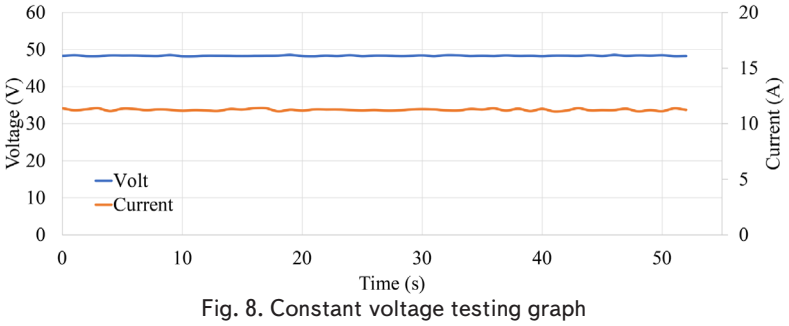

Fig. 8. Constant voltage testing graph

The first test on the integrated system aims to validate the bi-directional operational capability of the converter. In this scenario, the roles of the source and load are reversed: the 72 V battery serves as the primary power source, and the converter is tasked with stepping down the voltage (buck mode) and supplying power stably to the load at a constant voltage of 48 V. This test is a functional simulation of an emergency condition, in which the system must be able to utilize energy from the battery to supply power to an external load. Operational stability in this mode is visualized in Fig. 8, which shows the output voltage and current over time. The quantitative results of this test, which highlight the efficiency and accuracy of the system, are summarized in Table 6.

As shown in Fig. 8, the output voltage (blue line) was successfully maintained at a constant level close to the 48 V setpoint with minimal fluctuations during the test. The quantitative performance summarized in Table 6 further reinforces these findings. The system was able to operate with a solid average efficiency of 91.42% and a very low average error of only 0.77% of the setpoint. Collectively, the stability shown in the graph and the high efficiency recorded in the table convincingly prove that this prototype is capable of working effectively in bi-directional mode, reliably supplying power from the battery to the load.

Table 6

Summary of converter performance in constant voltage mode as a power supply

Parameters	Value
Input voltage	72 V battery
Output voltage setpoint	48 V
Average efficiency	91%
Average voltage error	0.77%

After proving that the device is capable of operating reliably in power supply mode, peak testing was performed to validate the core function of the proposed solution: the system's ability to automatically and seamlessly switch from normal charging mode to emergency power supply mode. This mode transition process, triggered by a simulated primary power source failure, is documented visually in Fig. 9.

Fig. 9 presents empirical evidence of the successful functionality of the automatic mode transition. In the initial stage (left side), the system operates in normal MSCC charging mode, as indicated by stable V_{OUT_CC} voltage and I_{OUT_CC} current. Then, a primary power source failure is simulated by slowly decreasing the supply voltage.

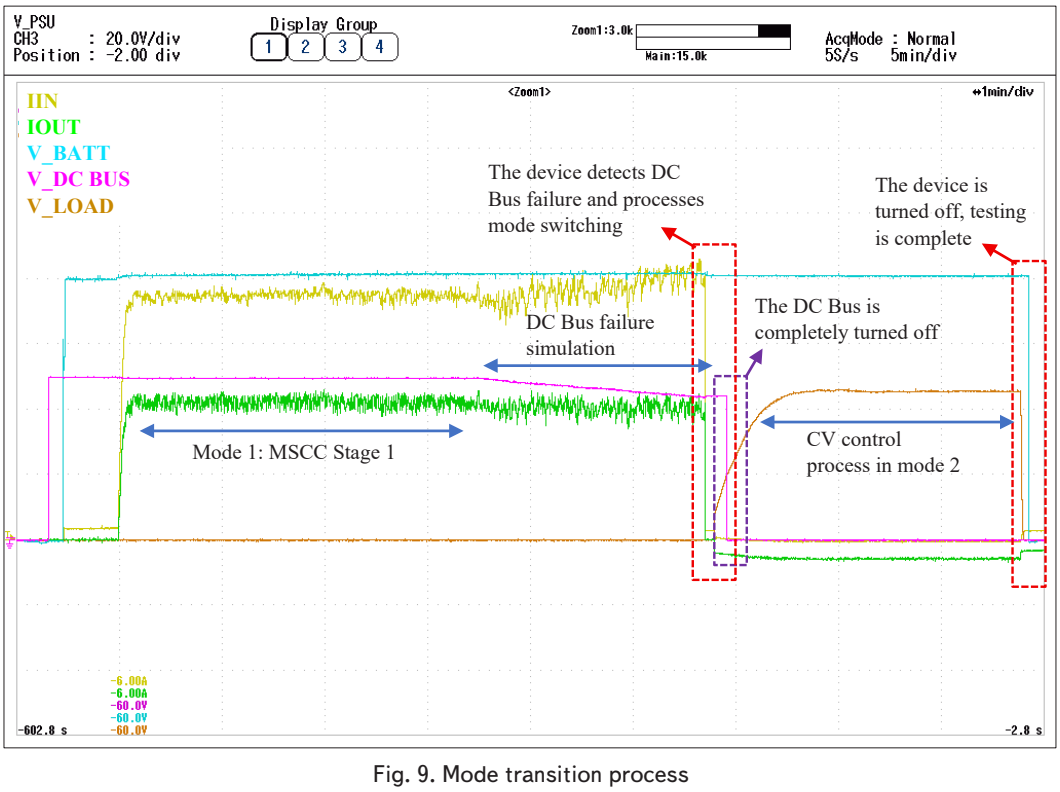

Fig. 9. Mode transition process

The graph shows how the device reacts to this disturbance by attempting to re-stabilize the charging current. When the supply voltage reaches a predetermined tolerance limit, the system automatically triggers a mode transition. This smooth transition is marked by the termination of the charging process and the activation of the emergency power supply mode. In the final stage (right), the V_lamp graph shows that the device successfully took over and supplied a stable constant voltage to the load, using the battery as its power source. The success of this fast and stable transition convincingly validates the core solution concept proposed in this study to improve the reliability of BSS.

Overall, the tests presented in this sub-section have successfully validated the full functionality of the integrated prototype. The test results convincingly demonstrate two core capabilities of the system: the ability to operate bi-directionally as a reliable power supply, and most importantly, the ability to automatically and seamlessly switch modes from normal charging to emergency mode in the event of a power source failure. The success of this functionality validation directly demonstrates that the proposed solution is capable of addressing the main research problem, namely improving the reliability and resilience of BSS against power disturbances. Thus, this prototype has been proven to be not only a collection of high-performance individual components, but also a functional integrated system that successfully validates the proposed solution concept.

To position the contribution of this research within the existing literature, a performance comparison with several relevant studies discussing similar topologies or related objectives is presented in Table 7. This table quantitatively compares key parameters such as power capacity, efficiency, and current ripple to highlight the advantages and novelty of the developed system.

As shown in Table 7, this study provides several significant unique contributions. Compared to previous research [37], the validation of two-way operation in this study was not only successful, but also at a power level 44 times higher (1100 W vs. 25 W) with far superior efficiency (93.44% vs. ~ 82%) and 8 times lower current ripple. Unlike other studies which main focus is on topology optimization to reduce the number of switch components [12], this study focuses on providing a functional integrated system solution for the reliability of BSS, an application context that was not the focus of those studies. Furthermore, although the potential for charging time savings has been successfully demonstrated through simulation [38], this study goes further by proving the effectiveness of the MSCC and FLC methods through implementation and testing on a real hardware prototype. Thus, the main contribution of this research is the design and validation of a high-performance integrated system that specifically addresses the challenge of operational reliability at BSS, which is a research gap that has not been widely explored.

Table 7

Comparison of research contributions with relevant literature

Study	Topology	Power (W)	Efficiency (%)	Iout Ripple (%)	Main contribution
[This Study]	Interleaved Bi-Dir. Non-Inv. Buck-Boost	1100	93.44	1	High-performance integrated solutions for BSS reliability
[37]	Cascaded Bi-Dir. Buck-Boost	25	81–83	8	Validation of bidirectional operations
[12]	Multiphase Cascaded Non-Inv. Buck-Boost	375	98.5	Not mentioned	Reduced switch count interleaved buckboost topology for dc-dc and ac-dc conversion systems
[38]	Buck-Boost with CC-Fuzzy	144	Not mentioned	Design: 20	Faster charging (12.5–25%) with FLC (simulation)

Overall, Chapter 5 has presented a series of experimental test results that systematically validate every aspect of the proposed system. It has been proven that, first, the interleaved converter hardware successfully doubles the power capacity while significantly reducing current ripple by 47.7%. Furthermore, the FLC-MSCC control algorithm has been proven to accelerate charging time by 13.7% compared to conventional methods. Most importantly, the validated integrated prototype is capable of operating bi-directionally and transitioning to emergency power supply mode smoothly and automatically. This collection of quantitative and qualitative results provides a strong empirical foundation for further discussion of the implications, advantages, and contributions of this research in the next chapter.

6. Discussion of performance analysis and implications for BSS operational reliability

The experimental results comprehensively validate the success of the proposed system, from its hardware performance to its functionality as an integrated solution for BSS reliability. The foundation of this system, the bi-directional interleaved converter, proved highly effective. This hardware topology is what explains the system's ability to double the power handling capacity to over 1.1 kW while maintaining a very high average operational efficiency of 93.44%, as detailed in Table 3. More importantly, the most significant advantage demonstrated by this topology is its ability to drastically reduce the output current ripple by 47.7% down to an average of only 0.92%, a finding quantified in Table 4. This dramatic reduction is a direct result of the ripple-cancellation effect inherent to the parallel interleaved design, a critical achievement as low current ripple is a key factor in maintaining battery health and extending its cycle life, a vital consideration for the expensive and essential components within a BSS ecosystem.

Building upon this reliable hardware platform, the implementation of the FLC for the MSCC method also yielded outstanding results, achieving a significant 13.7% reduction in charging time compared to the conventional CC-CV method. The reason for this enhanced time efficiency is visually confirmed in the comparative graph in Fig. 7, which clearly illustrates how the MSCC approach successfully eliminates the inefficient and lengthy CV phase that constitutes the slow "tail end" of a standard CC-CV charge cycle. The successful execution of this strategy is attributed to the FLC's capability, visualized in Fig. 6, to precisely and stably regulate the transitions between the distinct current stages (4 A, 2.8 A, and 2 A). This capability directly translates to increased station throughput and improved business model viability for a BSS. The culmination of this research was the validation of the system's integrated functionality. The prototype successfully demonstrated reliable bi-directional operation and, most importantly, the ability to perform a seamless and automatic mode transition from normal charging to an emergency power supply mode during a simulated main power failure, as documented in the oscilloscope waveform in Fig. 9. This capability provides direct empirical evidence that the proposed

integrated solution effectively addresses the primary research problem: enhancing the operational reliability and resilience of a BSS against electrical grid disturbances.

When positioned against existing literature, as summarized in Table 7, the unique contribution of this research becomes evident. While previous studies have validated the concept of bidirectional operation, they were often conducted at significantly lower power levels with inferior efficiency and higher current ripple; for instance, this study achieved its results at a power level 44 times higher than that in [37] with far superior performance. Unlike other research that focused primarily on theoretical topology optimization to reduce switch component counts [12], this study delivers a complete, functional, and high-power integrated system with a clear application focus on BSS reliability. Furthermore, where some studies have demonstrated the potential for faster charging through simulation [38], this research advances the field by proving the effectiveness of the FLC-MSCC method through implementation and rigorous testing on a real hardware prototype, thus filling a critical gap left by previous work.

The limitations of the study are as follows. The validation was conducted within a controlled laboratory environment, and its long-term performance in a real-world, dynamic BSS setting remains to be tested. Furthermore, practical testing of the prototype revealed several design disadvantages that warrant improvement. A primary issue is the significant electromagnetic interference (EMI) generated during the converter's high-frequency operation, which was observed to disrupt UART data communication between the microcontroller and its RS485 transceiver. Additionally, the current thermal management design proved to be suboptimal, with thermal measurements indicating hotspots of up to 55°C around the main switching components, suggesting inadequate heat dissipation. The logical development of this research would involve not only moving towards field trials but also refining the hardware design based on these findings. The primary difficulty anticipated will be experimental and logistical, involving the integration of a more robust hardware version into a live, commercial infrastructure.

7. Conclusions

1. The interleaved bi-directional non-inverting buck-boost converter was successfully designed and validated, demonstrating superior hardware performance. The implementation of this topology doubled the power handling capacity to 1.1 kW and, more critically, suppressed the output current ripple by 47.7% to a minimal 0.92%. This significant ripple reduction is attributed to the inherent ripple-cancellation effect of the parallel interleaved structure, which is a crucial factor for preserving long-term battery health and cycle life in BSS applications.

2. The FLC for the MSCC charging method was effectively implemented and evaluated, proving its superiority in charging time efficiency. The proposed FLC-MSCC method achieved a 13.7% reduction in total charging duration compared to the conventional CC-CV technique. This time-saving advantage stems from the elimination of the inefficient CV phase, as the FLC intelligently modulates the current in distinct stages to maintain an optimal power transfer rate, thereby enhancing the operational throughput of the BSS.

3. The integrated system's core functionality was fully validated, confirming its capability for both reliable bi-directional operation and, most importantly, a seamless automatic transition from standard charging to emergency power supply mode upon a primary power source failure. This robust transition is governed by the embedded control logic that actively monitors the main bus voltage and actuates relays to reroute power flow from the battery to the load. This successful validation provides direct empirical evidence that the proposed integrated solution effectively addresses the critical challenge of operational reliability in BSS, representing the primary contribution of this research by filling a distinct gap in the literature for hardware-verified, high-performance resilience systems.

Conflict of interest

The authors declare that they have no conflict of interest in relation to this study, whether financial, personal, authorship or otherwise, that could affect the study and its results presented in this paper.

Financing

This study was financially supported by the Directorate of Commercialization and Partnership, Directorate General of Research and Development, Ministry of Higher Education, Science, and Technology of the Republic of Indonesia.

Data availability

Data cannot be made available for reasons disclosed in the data availability statement.

Use of artificial intelligence

The authors have used artificial intelligence technologies within acceptable limits to provide their own verified data, which is described in the research methodology section.

Acknowledgments

The authors gratefully acknowledge the Directorate of Commercialization and Partnership, Directorate General of Research and Development, Ministry of Higher Education, Science, and Technology of the Republic of Indonesia, for its support and facilitation throughout the implementation of this research and publication process.

References

1. Asy'ari, M. K., Panggabean, D. K. S. H., Musyafa, A., Ginting, K. B. (2025). Development of a lithium-ion battery charging system under constant current and voltage conditions using STM-32 based on fuzzy logic control. Indonesian Physical Review, 8 (1), 340–348. https://doi.org/10.29303/ipr.v8i1.409

2. Yousuf, A. K. M., Wang, Z., Paranjape, R., Tang, Y. (2023). Electric Vehicle Charging Station Infrastructure: A Comprehensive Review of Technologies, Challenges, and Mitigation Strategies. 2023 IEEE Canadian Conference on Electrical and Computer Engineering (CCECE), 588–592. https://doi.org/10.1109/ccece58730.2023.10289005
3. Siddiqua, A., Cherala, V., Yemula, P. K. (2023). Optimal Sizing and Adaptive Charging Strategy for the Battery Swapping Station. 2023 IEEE PES 15th Asia-Pacific Power and Energy Engineering Conference (APPEEC), 1–6. https://doi.org/10.1109/appeec57400.2023.10561997
4. Afshar, S., Macedo, P., Mohamed, F., Disfani, V. (2020). A Literature Review on Mobile Charging Station Technology for Electric Vehicles. 2020 IEEE Transportation Electrification Conference & Expo (ITEC), 1184–1190. https://doi.org/10.1109/itec48692.2020.9161499
5. Reddy, N. A., Shreyash, K. S., Adithya, N. V., Namitha, D., Kalyan, C. P. (2023). Integration and Implementation of Renewable Energy based Charging Station. 2023 First International Conference on Cyber Physical Systems, Power Electronics and Electric Vehicles (ICPEEV), 1–5. https://doi.org/10.1109/icpeev58650.2023.10391903
6. Teske, P., Gentejohann, M., Wiemann, D., Krüger, L., Kowal, J., Dieckerhoff, S. (2024). Open Battery Platform: Open-Source Power Electronic Devices for Renewable Generation and Energy Storage Technology. 2024 IEEE 15th International Symposium on Power Electronics for Distributed Generation Systems (PEDG), 1–6. https://doi.org/10.1109/pedg61800.2024.10667440
7. Kumar, R., Verma, M., Kulkarni, A. (2024). Optimizing Bidirectional EV Charger with Rapid Charging Architecture using Fuzzy Logic Control. 2024 3rd International Conference for Innovation in Technology (INOCON), 1–6. https://doi.org/10.1109/inocon60754.2024.10511811
8. Sharma, A., Veerachary, M. (2018). A DC-DC Bidirectional Converter with Improved Mode Transition Technique. 2018 IEEE International Conference on Power Electronics, Drives and Energy Systems (PEDES), 1–6. https://doi.org/10.1109/pedes.2018.8707722
9. Schaltz, E., Rasmussen, P. O., Khaligh, A. (2008). Non-inverting buck-boost converter for fuel cell applications. 2008 34th Annual Conference of IEEE Industrial Electronics. https://doi.org/10.1109/iecon.2008.4758065
10. Rao, A. V., Guruswamy, K. P. (2021). Analysis, Design and Simulation of Non-Inverting Buck-Boost DC-DC Converter for Battery Charging. 2021 International Conference on Disruptive Technologies for Multi-Disciplinary Research and Applications (CENTCON), 79–84. https://doi.org/10.1109/centcon52345.2021.9688165
11. Polat, H., Hosseinabadi, F., Hasan, Md. M., Chakraborty, S., Geury, T., El Baghdadi, M. et al. (2023). A Review of DC Fast Chargers with BESS for Electric Vehicles: Topology, Battery, Reliability Oriented Control and Cooling Perspectives. Batteries, 9 (2), 121. https://doi.org/10.3390/batteries9020121
12. Abdel-Rahim, O., Chub, A., Blinov, A., Vinnikov, D., Peftitsis, D. (2022). An Efficient Non-Inverting Buck-Boost Converter with Improved Step Up/Down Ability. Energies, 15 (13), 4550. https://doi.org/10.3390/en15134550
13. Nguyen, V.-S., Tran, V.-L., Choi, W., Kim, D.-W. (2014). Analysis of the Output Ripple of the DC-DC Boost Charger for Li-Ion Batteries. Journal of Power Electronics, 14 (1), 135–142. https://doi.org/10.6113/jpe.2014.14.1.135
14. Alharbi, M. A., Alcaide, A. M., Dahidah, M., P., M.-R., Ethni, S., Pickert, V., Leon, J. I. (2023). Rotating Phase Shedding for Interleaved DC–DC Converter-Based EVs Fast DC Chargers. IEEE Transactions on Power Electronics, 38 (2), 1901–1909. https://doi.org/10.1109/tpel.2022.3211864
15. Zhang, C., Xu, B., Jasni, J., Radzi, M. A. M., Azis, N., Zhang, Q. (2022). Model Control and Digital Implementation of the Three Phase Interleaved Parallel Bidirectional Buck–Boost Converter for New Energy Electric Vehicles. Energies, 15 (19), 7178. https://doi.org/10.3390/en15197178
16. Pirashanthiyah, L., Edirisinghe, H. N., De Silva, W. M. P., Bolonne, S. R. A., Logeeshan, V., Wanigasekara, C. (2024). Design and Analysis of a Three-Phase Interleaved DC-DC Boost Converter with an Energy Storage System for a PV System. Energies, 17 (1), 250. https://doi.org/10.3390/en17010250
17. Suryoatmojo, H., Pratama, I. A., Soedibyo, S. (2021). Non-Inverting Cascaded Bidirectional Buck-Boost DC-DC Converter with Average Current Mode Control for Lithium-Ion Battery Charger. JAREE (Journal on Advanced Research in Electrical Engineering), 5 (2). https://doi.org/10.12962/jaree.v5i2.167
18. Alajmi, B. N., Marei, M. I., Abdelsalam, I., Ahmed, N. A. (2022). Multiphase Interleaved Converter Based on Cascaded Non-Inverting Buck-Boost Converter. IEEE Access, 10, 42497–42506. https://doi.org/10.1109/access.2022.3168389
19. Sunarno, E., Suhariningsih, Prasetyono, E., Nugroho, M. A. B., Eviningsih, R. P., Nizar, R. F. (2024). Interleaved Buck Converter as Current Regulator for Lithium Ion Battery Charging with Fuzzy Logic Control. 2024 International Electronics Symposium (IES), 13–18. https://doi.org/10.1109/ies63037.2024.10665860
20. Batteries in a Portable World (2017). Isidor Buchmann. Available at: https://batteryuniversity.com/buy-the-book.
21. Nugroho, M. A. B., Alifi, A. D., Suhariningsih, S., Sunarno, E., Prasetyono, E., Anggriawan, D. O. (2024). Multi-step constant current-constant voltage charging method to improve CC-CV method on lead acid batteries. TELKOMNIKA (Telecommunication Computing Electronics and Control), 22 (6), 1564. https://doi.org/10.12928/telkomnika.v22i6.25968
22. Imran, R. M., Li, Q., Flaih, F. M. F. (2020). An Enhanced Lithium-Ion Battery Model for Estimating the State of Charge and Degraded Capacity Using an Optimized Extended Kalman Filter. IEEE Access, 8, 208322–208336. https://doi.org/10.1109/access.2020.3038477

23. Khan, A. B., Pham, V.-L., Nguyen, T.-T., Choi, W. (2016). Multistage constant-current charging method for Li-Ion batteries. 2016 IEEE Transportation Electrification Conference and Expo, Asia-Pacific (ITEC Asia-Pacific), 381–385. https://doi.org/10.1109/itec-ap.2016.7512982
24. Khan, A. B., Choi, W. (2018). Optimal Charge Pattern for the High-Performance Multistage Constant Current Charge Method for the Li-Ion Batteries. IEEE Transactions on Energy Conversion, 33 (3), 1132–1140. https://doi.org/10.1109/tec.2018.2801381
25. Balamurugan, P., Agarwal, P., Khajuria, D., Mahapatra, D., Angalaeswari, S., Natrayan, L., Mammo, W. D. (2023). State-Flow Control Based Multistage Constant-Current Battery Charger for Electric Two-Wheeler. Journal of Advanced Transportation, 2023, 1–11. https://doi.org/10.1155/2023/4554582
26. Yurkovich, S., Passino, K. M. (1999). A laboratory course on fuzzy control. IEEE Transactions on Education, 42 (1), 15–21. https://doi.org/10.1109/13.746327
27. Shekhar, Y., Verma, S., Singh, N., Mishra, P., Ahmad, A. U., Bharati, K. K. (2024). Smart Control Strategies in Photovoltaic Systems: A Critical Review on Fuzzy Logic MPPT And PI Control For Charge Management. 2024 3rd International Conference on Power Electronics and IoT Applications in Renewable Energy and Its Control (PARC), 238–243. https://doi.org/10.1109/parc59193.2024.10486316
28. Falih, A. Z., Efendi, M. Z., Murdianto, F. D. (2021). CC-CV Controlled Fast Charging Using Fuzzy Type-2 for Battery Lithium-Ion. JAREE (Journal on Advanced Research in Electrical Engineering), 5 (2). https://doi.org/10.12962/jaree.v5i2.200
29. Faisal, M., Hannan, M. A., Ker, P. J., Hossain Lipu, M. S., Uddin, M. N. (2021). Fuzzy-Based Charging-Discharging Controller for Lithium-Ion Battery in Microgrid Applications. IEEE Transactions on Industry Applications, 57 (4), 4187–4195. https://doi.org/10.1109/tia.2021.3072875
30. Wiryajati, I. K., Satiawan, I. N. W., Suksmadana, I. M. B., Wiwaha, B. B. P. (2025). Investigation and Analysis of Fuzzy Logic Controller Method on DC-DC Buck-Boost Converter. Jurnal Penelitian Pendidikan IPA, 11 (1), 1066–1074. https://doi.org/10.29303/jppipa.v11i1.9744 Recommended External Circuitry for Transphorm GaN FETs (2018). Transphorm. Available at: https://www.mouser.com/pdfDocs/recommended-external-circuitry-transphorm-gan-fets-20190711-5.pdf?srsltid=AfmBOoqZ34XYpr2Q3s6cxq0_AcoadEeWW0I0yk4ZdjwhWCp1gheDbzZu
31. STM32G441xB. Datasheet (2021). STMicroelectronics. Available at: https://www.st.com/resource/en/datasheet/stm32g441cb.pdf